

Einstein-Podolsky-Rosen entanglement and steering in two-well Bose-Einstein-condensate ground states

Q. Y. He,^{1,2} P. D. Drummond,² M. K. Olsen,³ and M. D. Reid²

¹State Key Laboratory of Mesoscopic Physics, School of Physics, Peking University, Beijing 100871, China

²Centre for Quantum Atom Optics, Swinburne University of Technology, Melbourne, Victoria 3000, Australia

³Centre for Quantum Atom Optics, University of Queensland, Brisbane, Queensland 4072, Australia

(Received 3 January 2012; published 22 August 2012)

We consider how to generate and detect Einstein-Podolsky-Rosen (EPR) entanglement and the steering paradox between groups of atoms in two separated potential wells in a Bose-Einstein condensate. We present experimental criteria for this form of entanglement and propose experimental strategies for detecting entanglement using two- or four-mode ground states. These approaches use spatial and/or internal modes. We also present higher-order criteria that act as signatures to detect the multiparticle entanglement present in this system. We point out the difference between spatial entanglement using separated detectors and other types of entanglement that do not require spatial separation. The four-mode approach with two spatial and two internal modes results in an entanglement signature with spatially separated detectors, conceptually similar to the original EPR paradox.

DOI: [10.1103/PhysRevA.86.023626](https://doi.org/10.1103/PhysRevA.86.023626)

PACS number(s): 03.75.Gg, 03.75.Dg, 67.85.Fg, 67.85.De

I. INTRODUCTION

The Einstein-Podolsky-Rosen (EPR) paradox [1] established a link between entanglement and nonlocality [2] in quantum mechanics. The extent to which entanglement can exist in spatially separated macroscopic and massive systems is still essentially unknown. EPR entanglement in optics, however, has been extensively studied and numerous experiments have shown evidence for it [3–8]. An important distinction is that optical entanglement involves (nearly) massless particles and hence is a much less rigorous test of any gravitational decoherence effects present.

The generation of EPR entanglement between two massive systems therefore represents an important challenge. Such entanglement is a step in the direction of fundamental tests of quantum mechanics and is relevant to the long-term quest for understanding the relationship between quantum theory and gravity [9]. Ultimately, one would like to demonstrate spatially entangled mass distributions and this appears much more promising for ultracold atoms than for room-temperature atoms. For this reason we focus on ultracold Bose-Einstein condensate (BEC) environments here. Demonstration of mass entanglement is also relevant if BEC interferometry is to be useful to those areas of quantum information and metrology where entanglement is known to give an advantage [10–16]. In this paper we study strategies for the generation of EPR entanglement between Bose-Einstein condensates confined to two spatially separated potential wells.

Quantum correlations and EPR tests for Bose-Einstein condensates have been suggested previously, with strategies involving molecular down-conversion [17] and four-wave-mixing interactions [18–20], among others. Early experiments measuring free-space correlations demonstrated promising signatures of increased fluctuations associated with entanglement [21,22], but were unable to conclusively demonstrate entanglement or squeezing of quantum noise via reduced fluctuations, largely due to measurement inefficiencies. This has improved with recent multichannel-plate detection methods, but detection efficiency still remains an issue [23].

Entanglement and twin matter wave squeezing have also been measured very recently for distinct but nearly spatially superimposed modes in an optical lattice [24–26].

Here we are motivated to study the two-well case in view of experiments that have used this or similar systems to confirm both subshot-noise quantum correlations [27] and multiparticle entanglement among a small group of atoms [28,29]. For much larger numbers of atoms ($\sim 40\,000$) nearly quantum limited interferometry has been recently verified [30], showing that trapped atom interferometry has the potential to reach mesoscopic sizes. There have also been a number of previous theoretical studies [31,32] that outline different proposals and entanglement signatures.

The goal of this paper is to first clarify what it means to have an EPR entanglement between groups of atoms in a BEC and to then outline a strategy for achieving this goal. We define EPR entanglement as entanglement existing between two spatially separated systems so that an EPR paradox can be realized. For EPR entanglement to be claimed, three properties must be evident [7].

(i) Two systems are shown to be entangled through local measurements at spatially distinct locations.

(ii) The nature of the entanglement criterion confirms an EPR paradox. This requires measurement of sufficiently strong correlation between the two systems for two noncommuting EPR observables such as position and momentum, conjugate spins, or conjugate quadrature phase amplitudes [8]. A generalized approach would allow other entanglement measures such as those for EPR steering [33–40], which reveal an inconsistency between Einstein-Podolsky-Rosen’s local realism and the completeness of quantum mechanics using more general measurement strategies.

(iii) To fully justify the EPR no “spooky action-at-a-distance” assumption [1], the measurement events should be spacelike separated [2,4,5].

For large groups of atoms, the task of detecting EPR entanglement is much more feasible when the emphasis is on the EPR paradox itself rather than on the failure of Bell’s local hidden-variable model [2]. This leaves room for the possibility

of confirming multiparticle entanglement, a subject we touch on briefly in this paper. For spatially separated systems the detection of a sufficient correlation of locally defined EPR observables so that entanglement is confirmed [41–43] would represent an achievable first benchmark. This by itself is not direct evidence for the EPR paradox, or quantum steering, although it is a necessary condition. The second step (ii) of confirming the paradox has been carried out for photons [7] and also appears achievable for atoms. The last step (iii) is probably the most difficult for atoms. It would require either very fast measurements in one vacuum chamber or hybrid techniques involving two separated BECs with coupling via atom-photon interfaces [44] in order to achieve causally separated measurement.

There are many possible strategies for the generation of spatial EPR entanglement. Early experiments employed two-photon cascades and later optical parametric down-conversion to generate entangled photon pairs [3–5]. Continuous-variable EPR entanglement between two fields in a so-called two-mode squeezed state [45] was also generated using parametric down-conversion [6,8,46]. Such entanglement gave evidence for an EPR paradox [7], although true causal separation of measurement events was not demonstrated in these experiments.

The paper is arranged as follows. In Sec. II we outline possible entanglement strategies. Section III focuses on signatures for demonstrating entanglement, including nonlocality measures such as steering [34] and Bell’s nonlocality [2], as well as signatures for detecting multiparticle entanglement. Section IV considers entanglement preparation in a two-well system, modeled as two modes with boson operators a and b [47]. In this case the S -wave scattering intrawell interactions, given by Hamiltonians $H/\hbar = ga^{\dagger 2}a^2$ and $gb^{\dagger 2}b^2$, provide a local nonlinearity at each well, while the coupling (or tunneling) interwell term, modeled as $H/\hbar = \kappa(a^{\dagger}b + ab^{\dagger})$, generates interwell entanglement. Here the intrawell and interwell interactions act simultaneously to enhance entanglement formation in the ground state. Section V treats a four-mode generalization of this, which has the advantage that EPR entanglement can be measured using atom counting at each site, without the use of a local oscillator. Our conclusions are summarized in Sec. VI, with details given in the Appendix. This paper is based on preliminary work presented in a Letter [32].

II. ENTANGLEMENT STRATEGIES

A. Prototypical states for two-mode entanglement

Suppose two spatially separated systems are describable as distinct modes, represented by boson operators a and b . There are two processes that one can consider that can give multiparticle EPR entanglement. The first, which we call particle-pair generation, is currently the most widely known and used [6]. We consider an entangled state with number correlations

$$|\psi\rangle_I = \sum_{n=0}^{\infty} c_n |n\rangle_a |n\rangle_b. \quad (1)$$

This type of two-mode squeezed state gives two-particle correlations arising from a pair-production process $H/\hbar = \kappa a^{\dagger}b^{\dagger} + \kappa^*ab$, where $\langle ab^{\dagger} \rangle = 0$ but $\langle ab \rangle \neq 0$, and the number difference is always squeezed [48,49]. These EPR states are formed in optics via parametric down-conversion [7,8], or nondegenerate four-wave mixing [50]. Since they are not number conserving, they are not typical of states formed in coupled two-well experiments, although they have been generated in recent BEC experiments using spin- or mode-changing collisions [24–26].

In this paper we will focus on a second form of EPR entanglement, which we call number conserving. This occurs, for example, when fixed number states are input into a beam splitter, as described by the Hamiltonian: $H/\hbar = \kappa(a^{\dagger}b + ab^{\dagger})$, so that $\langle ab \rangle = 0$ but $\langle ab^{\dagger} \rangle \neq 0$. We consider an entangled number-conserving state of the form

$$|\psi\rangle_{II} = \sum_{n=0}^N c_n |n\rangle_a |N-n\rangle_b. \quad (2)$$

This is a simple description of the state prepared in some recent two-well BEC experiments where the total number is conserved [27,28]. We will examine how to unambiguously detect two-mode entanglement and EPR steering entanglement for these states. An important advantage of this approach is that all the atoms in a condensate can be entangled, which is generally not possible in particle-pair methods due to quantum feedback and pump depletion [51] in the pair-production dynamics.

B. Experimental strategies

Before examining detailed solutions for an interacting BEC, it is useful to summarize in schematic form how two-mode number-conserving entanglement can be generated. We consider how to generate entanglement between two groups of atoms in separated potential wells in a BEC. What is useful is a combination of *nonlinear local* interactions to generate a nonclassical squeezed state in each well together with a *nonlocal linear* interaction to produce the entanglement between two spatially distinct locations. In the case of the BEC, the S -wave scattering can provide a nonlinear local interaction and quantum diffusion across a potential barrier acts like a beam splitter to provide the nonlocal linear interaction.

We show in Sec. IV that the entanglement generated for the two-well ground state with a fixed number of atoms can translate to an EPR steering type of entanglement [34,40] (Fig. 1). For an *actual* demonstration of this sort of EPR entanglement, however, one must use signatures that involve local measurements for two spatially separated observers (often called Alice and Bob) at sites A and B . One can use local oscillator (LO) measurements at each site that provide phase shifts or their equivalent between the measured and LO modes [19,25]. In Sec. V we propose an alternative though similar four-mode strategy, as shown in Fig. 2. We summarize the two types of gedanken experiments as follows.

(i) *Two-mode entanglement preparation and then analysis.*

The entangled state is generated as the two-mode ground state in a double-well potential (Fig. 1). Experimentally this appears relatively simple, involving evaporative cooling to

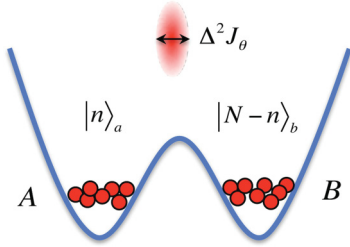


FIG. 1. (Color online) Two-mode case: a double-well one-spin-orientation BEC. The a and b are operators for two modes at A and B . The a and b are prepared with a two-mode number difference squeezing and an entanglement by adiabatic cooling to the ground state. We develop signatures to detect the interwell entanglement using interwell spin operators.

the ground state in a single well followed by an adiabatic ramping of an optical lattice to provide the central potential barrier [27,52]. However, there are two levels of experimental demonstration of the entanglement. The simplest involves a nonlocal measurement that recombines the two modes to demonstrate an interwell entanglement. For demonstration of the EPR steering paradox, however, strictly local measurements must be used. Einstein-Podolsky-Rosen steering entanglement can be detected with a phase-sensitive local oscillator measurement at each well, though this may represent an experimental challenge. This strategy is discussed in Sec. IV.

(ii) *Four-mode entanglement preparation and then analysis.* We consider four-mode states created through cooling in a double-well potential with two spin states in each well (Fig. 2). Experimentally this is more complex, but an EPR steering entanglement can be demonstrated using local Rabi rotations of the two spins of each well. This strategy is discussed in Sec. V.

In both the two- and four-mode cases, the basic idea is (a) correlated ground-state preparation through evaporative cooling in a potential well with linear coupling between wells; (b) local Rabi rotation (in the four-mode case) to a superposition of internal spins, thus choosing an EPR measurement

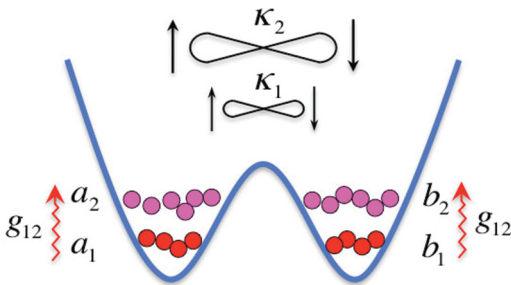


FIG. 2. (Color online) Four-mode case: a double-well two-spin-orientation BEC. We suppose the modes a_i and b_i are spatially separated. Modes a_1 and a_2 could be different spatial modes or different spin components of the same well. The pair a_1, b_1 (and a_2, b_2) can become entangled due to the interwell couplings. We allow for the asymmetric case where the pair a_2, b_2 has much greater numbers than a_1, b_1 ($N_2 \gg N_1$) and also consider a case where modes a_2 and b_2 need not be entangled ($\kappa_2 = 0$).

angle (in the two-mode case entanglement can be detected by a nonlocal rotation of the spins); and (c) measurement, usually from absorption imaging, giving occupation numbers.

III. EINSTEIN-PODOLSKY-ROSEN ENTANGLEMENT AND STEERING CRITERIA

In the original EPR proposal [1] the paradox arose from correlations between the positions and momenta of two particles emitted from the same source. With optical or atomic Bose fields, one can define the quadrature phase amplitudes of the modes as $X_A = a^\dagger + a$ and $Y_A = (a^\dagger - a)/i$ and similarly for mode b . These have similar commutators to position and momentum in the particle system. The detection of a sufficient correlation between the quadratures will signify entanglement [41,42] and the EPR paradox [8], as analyzed recently for atoms by Gross *et al.* [25].

We find that the common approach of detecting the EPR correlation as a reduced variance [8,41] in the sums and differences of quadrature amplitudes is not so useful for the number-conserving entangled states (2). Instead we adapt the criteria proposed by Hillery and Zubairy [53] and Cavalcanti *et al.* [40,54–57]. Like most practical criteria to date, these methods are sufficient, but not necessary, for the detection of entanglement. It is usually the case that some criteria are better suited than others to detect entanglement in a given system. The limitations of measures of entanglement based on purity, for example, have been discussed recently by Chianca and Olsen [58].

A. Two-mode Hillery-Zubairy entanglement criterion

Two subsystems A and B are said to be entangled if the density operator ρ for the composite system cannot be expressed as a mixture of product states, i.e.,

$$\rho = \sum_R P_R \rho_A^R \rho_B^R \tag{3}$$

fails, where $\sum_R P_R = 1$ and $\rho_{A(B)}^R$ is a density operator for A (B). Consider where systems are single field modes with boson operators a and b , respectively. Hillery and Zubairy showed that the two modes a and b are entangled if [53]

$$|\langle a^m (b^\dagger)^n \rangle|^2 > \langle (a^\dagger)^m a^m (b^\dagger)^n b^n \rangle. \tag{4}$$

All separable states [defined as those for which Eq. (3) holds] satisfy $|\langle a^m (b^\dagger)^n \rangle|^2 \leq \langle (a^\dagger)^m a^m (b^\dagger)^n b^n \rangle$.

In Ref. [32] we suggested how to rewrite the criterion (4) for $m = n$. For any non-Hermitian operator Z , we consider the generalized variance, which must be non-negative:

$$\Delta^2 Z \equiv \langle (Z^\dagger - \langle Z^\dagger \rangle)(Z - \langle Z \rangle) \rangle = \langle Z^\dagger Z \rangle - \langle Z^\dagger \rangle \langle Z \rangle \geq 0. \tag{5}$$

Defining $Z = a^m (b^\dagger)^m$, we find it is always true (for any state) that

$$|\langle a^m b^{\dagger m} \rangle|^2 - \langle a^{\dagger m} a^m b^{\dagger m} b^m \rangle \leq \langle a^{\dagger m} a^m ([b^m, b^{\dagger m}] \rangle). \tag{6}$$

Thus the Hillery-Zubairy (HZ) criterion (4) confirms entanglement if

$$0 \leq E_{\text{HZ}}^{(m)} = 1 + \frac{\langle a^{\dagger m} a^m b^{\dagger m} b^m \rangle - |\langle a^m b^{\dagger m} \rangle|^2}{\langle a^{\dagger m} a^m (b^m b^{\dagger m} - b^{\dagger m} b^m) \rangle} < 1. \quad (7)$$

It is also possible to derive a criterion using the commutators for mode a . Hence the HZ entanglement criterion (7) is best written with the optimal choice of denominator corresponding to the minimum of $\langle a^{\dagger m} a^m (b^m b^{\dagger m} - b^{\dagger m} b^m) \rangle$ or $\langle b^{\dagger m} b^m (a^m a^{\dagger m} - a^{\dagger m} a^m) \rangle$. The first-order ($m = n = 1$) HZ criterion for entanglement becomes

$$0 \leq E_{\text{HZ}}^{(1)} = 1 + \frac{\langle a^{\dagger} a b^{\dagger} b \rangle - |\langle a b^{\dagger} \rangle|^2}{\min\{\langle a^{\dagger} a \rangle, \langle b^{\dagger} b \rangle\}} < 1. \quad (8)$$

B. Multiparticle entanglement criterion

The second-order HZ entanglement criterion is obtained by using the power $m = 2$ with the identity $[b^2, b^{\dagger 2}] = 4b^{\dagger}b + 2$. Entanglement is then observed if

$$0 \leq E_{\text{HZ}}^{(2)} = 1 + \frac{\langle a^{\dagger 2} a^2 b^{\dagger 2} b^2 \rangle - |\langle a^2 b^{\dagger 2} \rangle|^2}{\langle a^{\dagger 2} a^2 (4b^{\dagger}b + 2) \rangle} < 1. \quad (9)$$

We now show that the higher-order HZ entanglement criterion (7) with $m > 1$ enables detection of multiparticle entanglement. The criterion (9) can only be satisfied if there exists a nonzero probability that the system is in an entangled superposition state of the form

$$|\psi\rangle = c|n_A\rangle|n_B\rangle + d|n_A + m\rangle|n_B - m\rangle + \sum_{n,l} c_{nl}|n\rangle|l\rangle \quad (10)$$

(or that obtained by interchanging the states of A and B) where the amplitudes $c, d \neq 0$ but c_{nl} are unspecified. Here $|n_A\rangle|n_B\rangle$ is the product number state with n_A particles in subsystem A and n_B particles in subsystem B .

Proof. Any composite system A - B can be described by a density matrix $\rho = \sum_R P_R \rho_{\text{sep}}^R + \sum_{R'} P_{R'} \rho_{\text{ent}}^{R'}$, where ρ_{sep}^R and $\rho_{\text{ent}}^{R'}$ represent pure separable and entangled states, respectively. The higher-order HZ entanglement measure (4) with $m = n$ can therefore be written as a ratio

$$R = \frac{|\langle a^m (b^{\dagger})^m \rangle|^2}{\langle (a^{\dagger})^m a^m (b^{\dagger})^m b^m \rangle}, \quad (11)$$

where

$$\langle a^m (b^{\dagger})^m \rangle = \sum_R P_R \langle a^m (b^{\dagger})^m \rangle_R + \sum_{R'} P_{R'} \langle a^m (b^{\dagger})^m \rangle_{R'}$$

and

$$\begin{aligned} \langle (a^{\dagger})^m a^m (b^{\dagger})^m b^m \rangle &= \sum_R P_R \langle (a^{\dagger})^m a^m (b^{\dagger})^m b^m \rangle_R \\ &+ \sum_{R'} P_{R'} \langle (a^{\dagger})^m a^m (b^{\dagger})^m b^m \rangle_{R'}. \end{aligned}$$

Here $\langle O \rangle_R$ represents the expectation value of O for state ρ_R . Since for a separable state $R \leq 1$, we can see that if $\sum_{R'} P_{R'} \langle a^m (b^{\dagger})^m \rangle_{R'} = 0$, it is always the case that ρ predicts $R \leq 1$. In short, the higher-order entanglement $E_{\text{HZ}}^{(m)} < 1$ cannot be achieved unless there is a nonzero probability

$P_{R'}$ for a pure entangled state $\rho_{\text{ent}}^{R'}$ for which $\langle a^m (b^{\dagger})^m \rangle \neq 0$. Expanding $\rho_{\text{ent}}^{R'}$ in terms of the number state basis $|n_A\rangle|n_B\rangle$ yields the form $\rho_{\text{ent}}^{R'} = |\psi\rangle\langle\psi|$, where

$$|\psi\rangle = \sum_{n,l} c_{nl}|n\rangle_A|l\rangle_B. \quad (12)$$

We see immediately that $\langle a^m (b^{\dagger})^m \rangle$ is nonzero only if states of type $c|n_A\rangle|n_B\rangle + d|n_A + m\rangle|n_B - m\rangle$, where $c, d \neq 0$, are included in the expansion.

C. Measurement of higher-order moments

We note that the moments of type $\langle a b^{\dagger} \rangle$ can be measured as a linear combination of moments of the Hermitian observables X_A and P_A , and X_B and P_B (on substituting $a^{\dagger} = (X_A + iP_A)/2$ and $b^{\dagger} = (X_B + iP_B)/2$). The measurement of the higher-order moments requires more explanation. For $m = 2$ expansion gives

$$\begin{aligned} \langle a^2 b^{\dagger 2} \rangle &= \frac{1}{16} \left((X_A^2 - P_A^2 - iX_A P_A - iP_A X_A) \right. \\ &\quad \left. \times (X_B^2 - P_B^2 + iX_B P_B + iP_B X_B) \right), \end{aligned}$$

for which the cross terms involving noncommuting observables pose a problem. These moments can be measured, however, by defining the two rotated observables $X_A^{\pm} = (X_A \pm P_A)/\sqrt{2}$, which are directly measurable. Similar observables are defined for the mode B . Then we note that $X_A P_A + P_A X_A = X_A^{+2} - X_A^{-2}$, which gives a means to determine the cross-term moments. In this case we are assuming the validity of quantum mechanics in order to equate the moments so that while the method is useful for detecting entanglement, the case of detecting higher-order steering or Bell's nonlocality would require a deeper analysis [57]. The intensity correlations of type $\langle a^{\dagger 2} a^2 b^{\dagger 2} b^2 \rangle$ can be measured via the established techniques for detecting particle bunching and antibunching [59,60] and Cauchy-Schwarz number correlation [61].

D. Two-mode EPR steering criterion

Nonlocality can be revealed using criteria similar to Eq. (4). Entanglement itself does not imply an EPR steering paradox [1,8,34,38] nor violation of local hidden-variable theories (Bell's theorem) [40,54–57,62], which are seen as stronger forms of entanglement. In this paper we consider two sites only and focus on the entanglement and EPR steering cases since it has been shown that violation of the moment Bell inequality derived in Ref. [54] requires three or more sites [56].

The entanglement evident in the EPR paradox was discussed by Schrödinger [33], who introduced the term steering to describe the apparent action at a distance. Criteria for the observation of steering can be developed using the asymmetric local hidden-state separable model of Wiseman *et al.* [34]. Violation of this model reveals inconsistency of EPR asymmetric local realism with the completeness of quantum mechanics and thus may be thought of as a generalized EPR paradox [34,35,38]. The EPR paradox steering nonlocality has been realized experimentally in loophole-free and high-efficiency scenarios for optical qubits [37] and Gaussian states [6,7].

An EPR steering nonlocality is detected if

$$|\langle a^m b^{\dagger n} \rangle|^2 > \left\langle a^{\dagger m} a^m \left(\frac{b^{\dagger n} b^n + b^n b^{\dagger n}}{2} \right) \right\rangle. \quad (13)$$

The proof follows from straightforward application of methods is given in Ref. [40], which derived this EPR steering criterion for $m = n = 1$. This criterion can also be rewritten in terms of the HZ entanglement parameter (8) so that *EPR steering entanglement* is confirmed for $m = n$ if

$$0 \leq E_{\text{HZ}}^{(m)} = 1 + \frac{\langle a^{\dagger m} a^m b^{\dagger m} b^m \rangle - |\langle a^m b^{\dagger m} \rangle|^2}{\langle a^{\dagger m} a^m (b^m b^{\dagger m} - b^{\dagger m} b^m) \rangle} < \frac{1}{2}. \quad (14)$$

E. Two-mode spin entanglement and EPR steering criteria

It is convenient to quantify entanglement using spin-operator methods, the advantage being that for BEC two-well systems the variances of Schwinger spins have been measured in experiment [27]. Hillery and Zubairy [53] have written the first-order criterion (4) in terms of the variances of interwell Schwinger spins, defined as

$$\begin{aligned} J_{AB}^X &= (a^\dagger b + ab^\dagger)/2, \\ J_{AB}^Y &= (a^\dagger b - ab^\dagger)/2i, \\ J_{AB}^Z &= (a^\dagger a - b^\dagger b)/2, \\ J_{AB}^2 &= \hat{N}_{AB}(\hat{N}_{AB} + 2)/4, \\ \hat{N}_{AB} &= a^\dagger a + b^\dagger b, \end{aligned} \quad (15)$$

where the outcomes for \hat{N}_{AB} are fixed at N and the spin is fixed as $J = N/2$. The HZ entanglement criterion given by Eq. (8) for $m = n = 1$ can then be rewritten as

$$0 \leq E_{\text{HZ}}^{(1)} = \frac{(\Delta J_{AB}^X)^2 + (\Delta J_{AB}^Y)^2}{\langle \hat{N}_{AB} \rangle / 2} < 1. \quad (16)$$

Throughout this paper we will use the notation $\Delta^2 J \equiv (\Delta J)^2$ interchangeably to mean the variance of measurements of J . We recall from Eq. (14) that EPR steering is observed if

$$0 < E_{\text{HZ}}^{(1)} < 1/2. \quad (17)$$

It should be noted that this type of spin-operator variance has been measured experimentally [27] by observing the interference between the two modes on expanding the atomic clouds after turning the traps off. However, as we discuss later, this strategy cannot be readily interpreted in the EPR sense due to the lack of separation during measurement.

The best entanglement (for a fixed number of atoms N) as measured by Eq. (16) is given when the sum of the two variances of J_{AB}^X and J_{AB}^Y is minimized. This sum can never be zero, meaning that the ideal entanglement of $E_{\text{HZ}}^{(1)} = 0$ cannot be reached because the spins J_{AB}^X and J_{AB}^Y do not commute. However, the sum becomes asymptotically small for large N , in which case large noise appears in the third spin J_{AB}^Z . The lower bound for the sum of the two variances has been obtained by [63]

$$\frac{(\Delta J_{AB}^X)^2 + (\Delta J_{AB}^Y)^2}{J} \geq C_J/J, \quad (18)$$

with the coefficients C_J given in Ref. [63]. The reduction of the sum $(\Delta J_{AB}^X)^2 + (\Delta J_{AB}^Y)^2$ below the standard quantum

limit (given by $J = \langle \hat{N}_{AB} \rangle / 2$) is referred to as planar squeezing and represents the onset of HZ entanglement.

Inequalities of the type (18) are useful for inferring multiparticle entanglement. The level of entanglement as measured by $E_{\text{HZ}}^{(1)}$ can give information about how many atoms are involved in the entangled state. Since a large spin J can only be obtained where the number of atoms N is large, very small squeezing necessarily implies an entangled state with a large number N . A complete analysis is beyond the scope of the present paper. This type of approach was originally developed by Sorenson and Molmer [64], who explained how to infer a multiparticle entanglement from the level of reduction in the spin-squeezing variance of J^Z [28,29].

F. Four-mode spin EPR entanglement criteria

A true EPR experiment would involve coherent combination of second fields or condensates at each site, as depicted schematically in Fig. 2. To observe true EPR entanglement between sites A and B a useful procedure is to use two modes per EPR site. Local intrawell spin measurements are defined for well A as:

$$\begin{aligned} J_A^X &= (a_1^\dagger a_2 + a_2^\dagger a_1)/2, \\ J_A^Y &= (a_1^\dagger a_2 - a_2^\dagger a_1)/2i, \\ J_A^Z &= (a_2^\dagger a_2 - a_1^\dagger a_1)/2, \\ \hat{N}_A &= a_2^\dagger a_2 + a_1^\dagger a_1. \end{aligned} \quad (19)$$

Here $a_{1,2}$ are mode operators for different components of the same site, typically different spatial modes or different nuclear spins at each site. We also introduce the notation for the corresponding raising and lowering spin operators $J_A^\pm = J_A^X \pm iJ_A^Y$. Similar spin operators are defined for site B . The set (19) defines complementary observables that are locally measurable at each site using Rabi rotations and number-difference measurements [28]. Calculations of spin correlations at two sites can be carried out most simply on imaging on a micrometer scale and then dividing the imaged atoms into two halves for measurement purposes. A more sophisticated method is to add a time-dependent external potential to divide the condensate into two widely separated parts. While this gives results that depend on the potential, it provides a physical separation between the sites.

Having defined local spin operators, we now need to consider a suitable EPR entanglement measure. Previous authors [62,65–70] have derived HZ-type entanglement and EPR steering criteria that are expressed in terms of the effective local spin operators (19). Entanglement is confirmed if

$$|\langle J_A^+ J_B^- \rangle|^2 > \langle J_A^+ J_A^- J_B^+ J_B^- \rangle. \quad (20)$$

Criteria involving higher moments are also possible, but are not examined here. The HZ spin criterion can be rewritten using the procedure outlined in Ref. [32]. If we define $Z = J_A^+ J_B^-$, then one can show that $\Delta^2(Z^+ Z^-) = \langle J_A^+ J_A^- J_B^+ J_B^- \rangle - \langle [J_A^+, J_A^-] J_B^+ J_B^- \rangle - |\langle J_A^+ J_B^- \rangle|^2 \geq 0$. Thus

$$\begin{aligned} &|\langle J_A^+ J_B^- \rangle|^2 - \langle J_A^+ J_A^- J_B^+ J_B^- \rangle \\ &\leq \langle [J_A^-, J_A^+] J_B^+ J_B^- \rangle = 2\langle J_A^Z J_B^Z \rangle. \end{aligned} \quad (21)$$

Similarly, defining $Z^\dagger = J_A^- J_B^+$, one can show that

$$|\langle J_A^+ J_B^- \rangle|^2 - \langle J_A^+ J_A^- J_B^+ J_B^- \rangle \leq 2\langle J_A^+ J_A^- J_B^Z \rangle. \quad (22)$$

The spin entanglement criterion (20) becomes

$$E_{\text{HZ}}^{\text{spin}(1)} = \frac{\Delta^2(J_A^+ J_B^-)}{\min[2\langle J_A^Z J_B^+ J_B^- \rangle, 2\langle J_A^+ J_A^- J_B^Z \rangle]} < 1, \quad (23)$$

i.e., HZ-type spin entanglement is verified if $E_{\text{HZ}}^{\text{spin}(1)} < 1$.

We have derived the spin EPR steering inequalities based on Eq. (20) in a previous paper [62]. Einstein-Podolsky-Rosen steering is detected if

$$|\langle J_A^+ J_B^- \rangle|^2 > \langle [(J_A^X)^2 - (J_A^Y)^2 \pm J_A^Z][(J_B^X)^2 - (J_B^Y)^2] \rangle, \quad (24)$$

which can be rewritten as

$$0 \leq E_{\text{HZ}}^{\text{spin}(1)} = 1 + \frac{\langle J_A^+ J_A^- J_B^+ J_B^- \rangle - |\langle J_A^+ J_B^- \rangle|^2}{\min[2\langle J_A^Z J_B^+ J_B^- \rangle, 2\langle J_A^+ J_A^- J_B^Z \rangle]} < \frac{1}{2}. \quad (25)$$

We note the spin moments of Eqs. (23) and (25) are actually measured via the X and Y spin components, for example, using the expansion

$$\langle J_A^+ J_B^- \rangle = \langle J_A^X J_B^X - i J_A^X J_B^Y + i J_A^Y J_B^X + J_A^Y J_B^Y \rangle. \quad (26)$$

IV. GENERATION OF TWO-MODE ENTANGLEMENT

We next turn to the physical means to generate EPR entanglement and steering in two-mode physical systems. We focus here on the gedanken experiment of Fig. 1, with explicit spatial separation of the two modes.

A. Linear beam splitter with fixed number input states

Possibly the simplest number-conserving entangled state is obtained with a number-squeezed input, together with a beam splitter interaction

$$H/\hbar = \kappa a^\dagger b + \kappa^* a b^\dagger, \quad (27)$$

which models the exchange of atoms that can take place between wells. On defining output (a , b), input (a_{in}), and vacuum input (a_v) modes, one can write the beam splitter transformation as

$$\begin{aligned} a &= (a_{\text{in}} + a_v)/\sqrt{2}, \\ b &= (a_{\text{in}} - a_v)/\sqrt{2}. \end{aligned} \quad (28)$$

1. Single number state input

We first consider the simplest case of N atoms input to one port of the beam splitter (Fig. 3). This is equivalent to the linear interferometer case [28] in which a fixed number of atoms is initially in one BEC well and is then redistributed between wells via a number-conserving mechanism. Using Eq. (28), the final state is number conserving [Eq. (2)]:

$$|\text{out}\rangle = \sum_{n=0}^N c_n |n\rangle_a |N-n\rangle_b, \quad (29)$$

where $c_n = \sqrt{N!}/\sqrt{2^N n!(N-n)!}$. This state (29) is entangled for all N . The entanglement can be detected using the HZ entanglement measure (7). The superposition (29) clearly involves up to N particles and this multiparticle entanglement can be detected using the higher-order entanglement $E_{\text{HZ}}^{(m)}$ criteria (7). Higher-order (up to 4th) entanglement becomes evident in Fig. 4. This linear beam splitter method generates a relatively small degree of entanglement, however (see Fig. 4), which will later be compared with the much more significant entanglement obtainable using nonlinear BEC interactions.

2. Double number state input

We next consider a double Fock number state $|N\rangle|N\rangle$ incident on a beam splitter (Fig. 5) as a model for the case where there is initially a fixed, equal number of atoms in each well.

The output state after an exchange (interference) between the wells is

$$|\text{out}\rangle = \sum_{n=0}^N c_n |2n\rangle_a |2(N-n)\rangle_b, \quad (30)$$

where $c_n = (-1)^{N-n} \sqrt{(2n)!} \sqrt{[2(N-n)!]/[2^N n!(N-n)!]}$. In this case entanglement is again present, but cannot be detected via the first-order entanglement criterion (8).

Entanglement can, however, be detected via the second-order HZ entanglement criterion (9), which indicates an entanglement involving a superposition of number states different by two particles (proved in Sec. III B). The fourth-order entanglement $E^{(4)}$ is also evident, indicating superpositions involving states separated by four particles. The entanglement measure $E^{(2)}$ is sufficiently strong that EPR steering can also be confirmed via Eq. (14) with $m = n = 2$, as shown in Fig. 6, though this effect is diminished for higher N .

B. Nonlinear case: BEC ground state

We now examine how to enhance the entanglement over the linear case above by using a local number-conserving nonlinearity. We solve for the ground state of a two-component BEC (Fig. 1), as modeled according to the two-mode Hamiltonian introduced by Milburn *et al.* [10,47]:

$$H/\hbar = \kappa(a^\dagger b + ab^\dagger) + \frac{g}{2}[a^\dagger a^\dagger a a + b^\dagger b^\dagger b b]. \quad (31)$$

Here κ denotes the conversion rate between the two components, denoted by the mode operators a and b , and $g \propto a_{3D}$

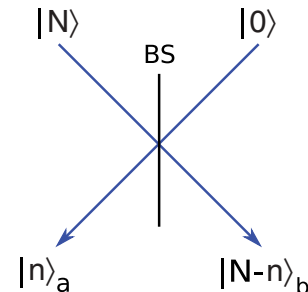


FIG. 3. (Color online) Fock number state $|N\rangle$ incident on a beam splitter (BS) produces an entangled state (2).

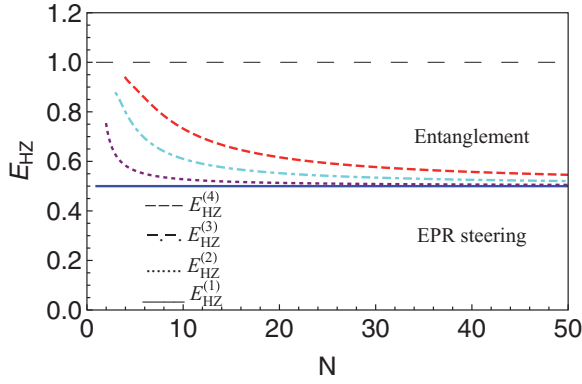


FIG. 4. (Color online) Entanglement of Fig. 3 detected by the HZ entanglement criterion ($E_{\text{HZ}} < 1$) [Eq. (7)]. Higher-order entanglement is indicated by the purple dotted, cyan dash-dotted, and red short dashed curves. The correlation does not confirm EPR steering entanglement from Eq. (14), which requires $E_{\text{HZ}} < 0.5$.

is the nonlinear self-interaction coefficient [47], proportional to the three-dimensional S -wave scattering length a_{3D} . The first term proportional to κ describes an exchange of particles between the two wells (modes) in which the total number is conserved. This term is the linear term equivalent to that for a beam splitter. We note here that at high densities it is necessary to also include nonlinear effects in this term [71]. The two-mode Hamiltonian model applies to many systems including optical cavity modes and superconducting waveguides with a nonlinear medium as well as to BECs [72].

The ground-state solution is obtained using standard matrix techniques and depends on the dimensionless ratio g/κ . We consider a total of N atoms: the number in well a is $\hat{N}_a = a^\dagger a$ and that in well b is $\hat{N}_b = b^\dagger b$.

Solutions show the generation of significant interwell two-mode entanglement, including multiparticle entanglement. The entanglement between modes a and b , and hence between the two wells, can be detected by the first-order HZ entanglement criterion $E_{\text{HZ}}^{(1)} < 1$ [Eq. (16)] for both attractive ($g < 0$) and repulsive ($g > 0$) regimes. Higher-order entanglement is also detectable. The results are summarized in Figs. 7 and 8.

1. Attractive interactions

The best first-order HZ entanglement (i.e., the smallest possible value for $E_{\text{HZ}}^{(1)}$) is given when the sum of the two

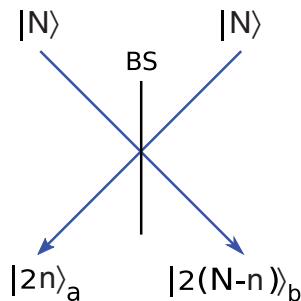


FIG. 5. (Color online) Double Fock number state incident on a beam splitter (BS) produces a number-conserving entangled state.

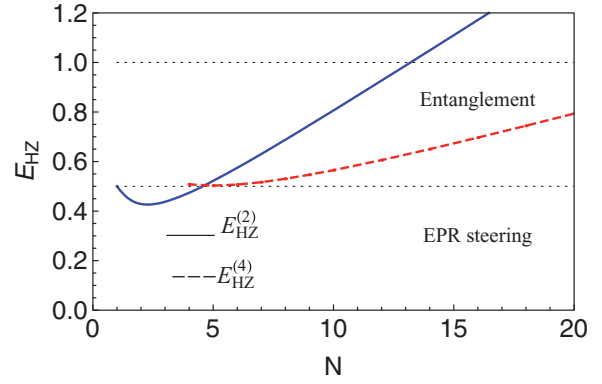


FIG. 6. (Color online) Hillery-Zubairy entanglement criterion using a double Fock number state and beam splitter. The graph shows the criterion (7) for $m = n = 2$ (solid blue line) and $m = n = 4$ (red dashed line). Einstein-Podolsky-Rosen, which requires $E_{\text{HZ}} < 0.5$ steering is observable with $m = n = 2$ and $N < 5$.

variances of J_{AB}^X and J_{AB}^Y of Eq. (16) is minimized. As explained in Sec. III E, this sum can never be zero.

The best first-order HZ intermode entanglement is predicted for the attractive regime ($g < 0$), which could be realized using ^{41}K and ^7Li isotopes. The absolute lower bound for $E_{\text{HZ}}^{(1)}$ is achieved for the ground state at a critical value $Ng_{11}/\kappa \approx -2.0$, as shown for $N = 100$ in Fig. 7 and for $N = 6$ in Fig. 8. This critical case has been studied and explained in Refs. [63,73]. We note that the minimum E_{HZ} becomes asymptotically small for large N . The maximum degree of HZ entanglement increases with N , the number of atoms, according to Eq. (18) and the relation for C_J obtained in Ref. [63]. The degree of entanglement is strong enough to give EPR steering.

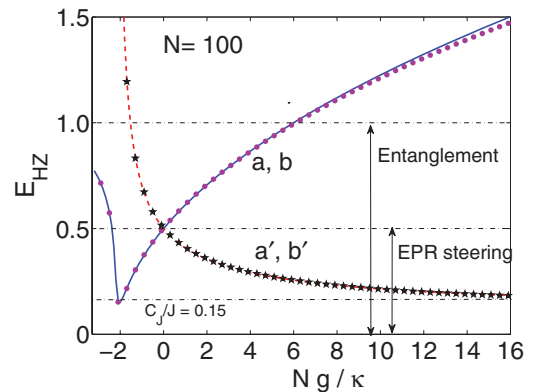


FIG. 7. (Color online) Entanglement in the ground state of the BEC Hamiltonian (31), using the HZ criterion (16), plotted against the coupling constant for both positive and negative couplings for $N = 100$ atoms. Plots show the first-order HZ entanglement as a function of Ng/κ , with $\kappa > 0$ held fixed and g varied. The mean spin is in the direction defined by J_{AB}^X . The HZ entanglement criterion $E_{\text{HZ}} < 1$ indicates a two-mode entanglement and $E_{\text{HZ}} < 0.5$ indicates EPR steering. The dashed red line gives the HZ criterion E'_{HZ} for the rotated modes a' and b' . The predictions for the respective second-order entanglement criterion $E_{\text{HZ}}^{(2)}$ [Eq. (9)] are given by the dotted and starred curves.

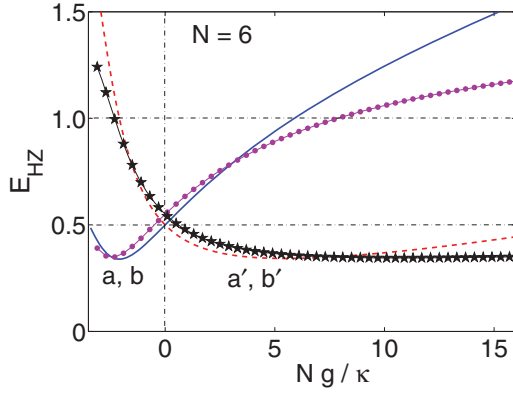


FIG. 8. (Color online) Same as Fig. 7 but for much lower particle number with $N = 6$. First-order entanglement $E_{\text{HZ}}^{(1)}$ in (a,b) is shown by the solid blue line; second-order entanglement $E_{\text{HZ}}^{(2)}$ is shown by the purple line with dots. First-order entanglement in (a',b') is shown by the dashed red line; second-order entanglement is shown by the black line with stars. The second-order entanglement criterion becomes more sensitive where the nonlinearity is higher.

The strongest theoretical entropic entanglement $\varepsilon(\rho)$ [74,75] is found for a pure state when all atom numbers are equally represented in the superposition. It is shown in Ref. [32] that the closest state to this optimum is obtained at a critical value of $Ng_{11}/\kappa \approx -2.0$, that is, the attractive interaction regime gives rise to a maximal spread in the distribution of numbers in each well.

Interestingly, Fig. 7 shows that the same point of maximum is observed for the higher-order entanglement measure $E_{\text{HZ}}^{(2)}$. This measure can only detect entanglement that originates from superpositions of the type

$$|50\rangle|51\rangle + |52\rangle|49\rangle \dots,$$

where at least some of the states of the superposition are separated by two quanta (proved in Sec. III B). Similarly, the third-order entanglement criterion $E_{\text{HZ}}^{(3)}$ would detect entanglement originating from states separated by three quanta. In the case of Fig. 7, where there are $N = 100$ quanta, the existence of entangled states such as $|0\rangle|100\rangle + \dots + |100\rangle|0\rangle$ could be detected in principle by measuring $E_{\text{HZ}}^{(100)} < 1$. This would give a possible strategy for detecting the entanglement of the NOON state (the superposition $|N\rangle|0\rangle + |0\rangle|N\rangle$), though measurement of the higher-order moments would present a challenge [76–80]. Further higher-order entanglement (e.g., $E_{\text{HZ}}^{(101)} < 1$) would not be possible where the total number of atoms fixed at $N = 100$.

2. Repulsive interactions

The repulsive regime ($g > 0$) also predicts considerable planar squeezing and entanglement (Fig. 7), but in that case the best planar squeezing is rotated into the X - Z plane as graphed in Fig. 9 [73,81]. A depiction of the resulting planar-squeezing ellipsoid is shown in Fig. 10.

Thus the corresponding HZ entanglement is between the modes defined by the *rotated* coordinates

$$a' = (a + b)/\sqrt{2}i, \quad b' = (a - b)/\sqrt{2}. \quad (32)$$

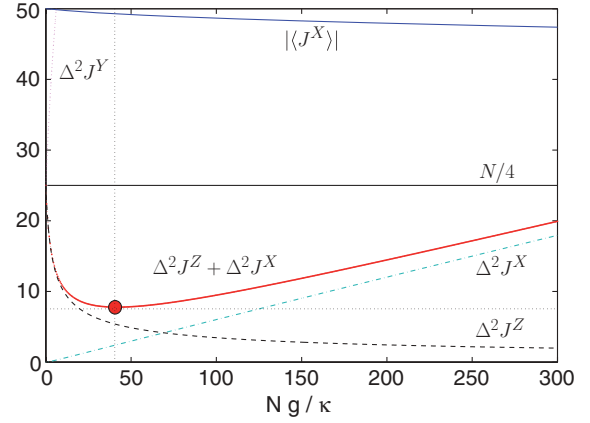


FIG. 9. (Color online) Repulsive interaction case for $N = 100$, showing individual spin variances and mean spin $|\langle J_{AB}^X \rangle|$ for the ground-state solution of the Hamiltonian (31) in the regime where there is a strong repulsive self-interaction g/κ for $N = 100$. Here $\kappa > 0$ is fixed and g is varied. Entanglement is obtained when $\Delta^2 J_{AB}^Z + \Delta^2 J_{AB}^X < N/2$ and squeezing of the individual spin J_{AB}^θ is obtained when $\Delta^2 J_{AB}^\theta < N/4$. For simplicity we have dropped the subscripts AB in the labeling of the variances in the figure. We note that the sum of the spin variances has a minimum value with a critical value of the coupling g/κ .

The corresponding entanglement criterion is given by

$$0 < E'_{\text{HZ}} = \frac{(\Delta J_{AB}^X)^2 + (\Delta J_{AB}^Z)^2}{(\langle a^\dagger a \rangle + \langle b^\dagger b \rangle)/2}. \quad (33)$$

The detection of spatial HZ entanglement between the two wells in the repulsive case would therefore require a different detection scheme, as proposed in Ref. [73]. We note that in both repulsive and attractive cases the HZ entanglement can be very significant, so the EPR steering nonlocality (14) is predicted via measurement of both the first- and second-order

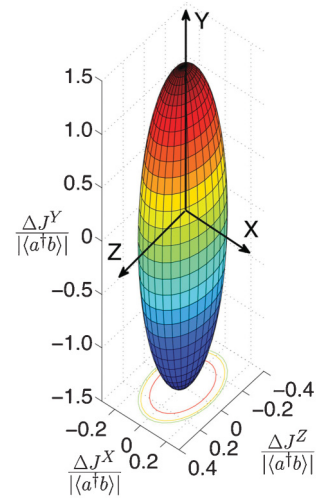


FIG. 10. (Color online) Three-dimensional variance ellipsoid corresponding to $N = 100$ and a repulsive interaction at the optimum coupling of $Ng/\kappa = 40$. Spin variances are reduced on both axes parallel to the X - Z plane to show strong but not perfect planar quantum squeezing. The variance increases perpendicular to the squeezing plane along the Y axis.

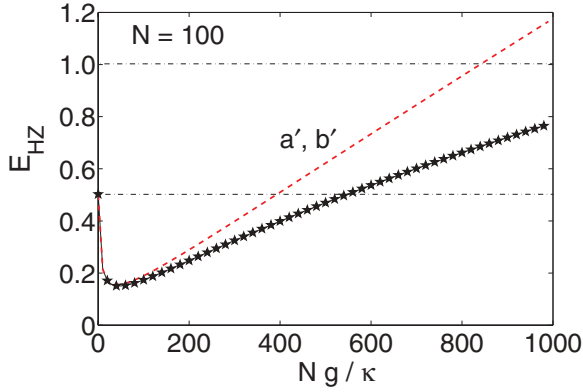


FIG. 11. (Color online) Higher-order entanglement for the case of $N = 100$. Other parameters are as in Fig. 7. Entanglement is obtained when $E_{\text{HZ}} < 1$. The red dashed line shows a reducing $E_{\text{HZ}}^{(1)}$ entanglement as g/κ is increased above a certain level. The solid black line (starred) shows the second-order entanglement measure $E_{\text{HZ}}^{(2)}$. The second-order entanglement $E_{\text{HZ}}^{(2)} < 1$ is achievable at higher g/κ ratios.

HZ moments. Figure 9 indicates that for fixed N the repulsive case shows an increasing and then reducing first-order HZ entanglement (8) as the nonlinearity g/κ increases. The optimum case for $N = 100$ and a repulsive interaction occurs at a coupling of $Ng/\kappa = 40$. The squeezing ellipsoid for this coupling is shown in Fig. 10.

Interestingly, however, from Fig. 11 we see that the second-order entanglement criterion for $N = 100$ detects more entanglement as the nonlinearity increases, suggesting that the drop in the entanglement measured by the first-order criterion is due to a change in the nature of the entanglement, that it involves superpositions of states with a greater number difference, as described in Sec. III B, rather than to a loss of entanglement itself. Figure 8 shows a similar behavior at much lower particle numbers ($N = 6$), although with less overall entanglement at the optimum coupling. In short, multiparticle entanglement is predicted to be detectable in the repulsive case for a wide range of parameter regimes.

We note that a second type of multiparticle entanglement can be inferred from the degree of first-order entanglement, as explained in Sec. III E. This approach was proposed in Ref. [64] and has been used to infer multiparticle entanglement in Bose-Einstein condensates [25,29] based on measurements of the variance of J_{AB}^Z . This second type of multiparticle entanglement puts a constraint on the minimum number of particles in the entangled state, but can include states such as

$$\{|50\rangle|50\rangle + |49\rangle|51\rangle\}/\sqrt{2}$$

and is therefore different from that inferred from the higher-order entanglement criteria involving $E_{\text{HZ}}^{(m)}$. Where the multiparticle entanglement is inferred from the first-order variances it is possible that the states making up the entanglement differ by only one particle number for each mode.

3. Measurement schemes

The spatial interwell entanglement can be confirmed, via E_{HZ} , from the measurements of the combined spins J_{AB} using interference measurements between the two condensates, as

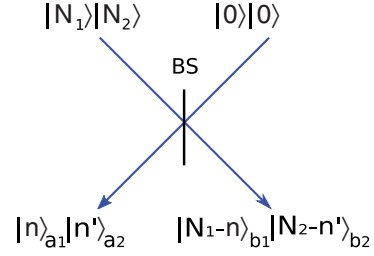


FIG. 12. (Color online) Pairs of Fock states transmitted through a beam splitter. The pair a_1, b_1 is coupled and becomes entangled, as does a_2, b_2 .

performed in Ref. [27]. Results obtained in this fashion are important in confirming the existence of entanglement within quantum theory, but as the measurements are not localized at each site, they cannot be viewed as rigorous tests of EPR entanglement, steering, or nonlocality. In order to use the above strategies to confirm an EPR-type entanglement one would measure the local EPR observables $X_{A(B)}$ and $P_{A(B)}$ at each well [19,24]. This is because the moments of Eq. (4) are in terms of the operators a and b , which are linear combinations of the Hermitian observables X and P . Optically, the X and P are measured using phase-sensitive local oscillators [6].

V. EINSTEIN-PODOLSKY-ROSEN ENTANGLEMENT: FOUR-COMPONENT CASE

We examine in this section how to use an additional mode per site to perform an effective local oscillator measurement in this BEC case. Similar strategies have been suggested by Ferris *et al.* [19].

A. Linear multimode case

We study the linear case first to model a fixed number of atoms with a minimal BEC nonlinear self-interaction. Suppose a Fock number state $|\psi_{\text{in}}\rangle = |N_1\rangle_{a_{\text{in}1}}|N_2\rangle_{a_{\text{in}2}}|0\rangle_{b_{\text{in}1}}|0\rangle_{b_{\text{in}2}}$ is incident on a beam splitter (Fig. 12) so that N_1 and N_2 are fixed and modes within each pair a_1, b_1 and a_2, b_2 are coupled by the beam splitter interaction, with a_1 and a_2 (and b_1 and b_2) remaining uncoupled. Output modes a_1 and b_1 are number conserved according to Eq. (2), as is the pair a_2, b_2 , and are given as $a_{1,2} = (a_{\text{in}1,2} + b_{\text{in}1,2})/\sqrt{2}$ and $b_{1,2} = (a_{\text{in}1,2} - b_{\text{in}1,2})/\sqrt{2}$, respectively. The output state is

$$|\text{out}\rangle = \sum_{n=0}^{N_1} \sum_{n'=0}^{N_2} c_{n,n'} |n\rangle_{a_1} |n'\rangle_{a_2} |N_1 - n\rangle_{b_1} |N_2 - n'\rangle_{b_2}, \quad (34)$$

where $c_{n,n'} = \sqrt{N_1!N_2!}/\sqrt{2^{N_1+N_2}n!(N_1-n)!n'!(N_2-n')!}$. We can evaluate moments to obtain the prediction for the HZ spin criterion (23). Figure 13 shows the result of varying N_1 for fixed $N_2 = 100$. The asymmetric case is favorable to detecting entanglement.

Where the initial state is more complex, such as $|\psi_{\text{in}}\rangle = |N_1\rangle_{a_{\text{in}1}}|N_2\rangle_{a_{\text{in}2}}|N_1\rangle_{b_{\text{in}1}}|N_2\rangle_{b_{\text{in}2}}$, the output state will involve superpositions of only even numbers of atoms in the symmetric and antisymmetric modes so that $|\langle J_A^+ J_B^- \rangle|^2 = |\langle a_2^\dagger a_1 b_2 b_1^\dagger \rangle|^2 = 0$. As in the case of Sec. IV A 2, we would detect this entanglement using an appropriate second-order spin criterion.

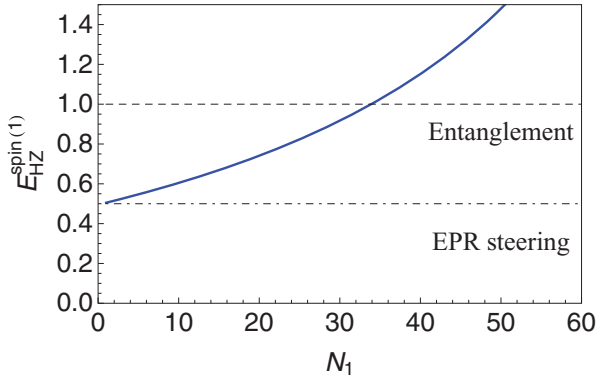


FIG. 13. (Color online) The entanglement of pairs of Fock states transmitted through a beam splitter can be detected via the spin Hillery-Zubairy criterion (23) for the asymmetric case where the pair a_2, b_2 has much greater numbers $N_2 \gg N_1$ ($N_2 = 100$). Entanglement is confirmed if $E_{\text{HZ}}^{\text{spin}(1)} < 1$.

B. Nonlinear four-component BEC case

We now consider the EPR entanglement that can be generated and measured when the modes interact to form the four-mode BEC ground state. We focus on setups that will enable the four-mode case to produce an EPR entanglement that is the replica of the two-mode HZ entanglement, as displayed in Figs. 7–11. In this case the second mode at each site may be thought of as part of a measurement system (Fig. 2).

1. Four-mode BEC Hamiltonian

We assume that the two-well four-mode system of Fig. 2 is described by the Hamiltonian [47,81]

$$H/\hbar = \sum_i \kappa_i a_i^\dagger b_i + \frac{1}{2} \left[\sum_{ij} g_{ij} a_i^\dagger a_j^\dagger a_j a_i \right] + \{a_i \leftrightarrow b_i\}. \quad (35)$$

We solve for the ground state of this Hamiltonian. We consider two modes at each EPR site A and B , with four modes in total, as shown schematically in Fig. 2. This corresponds to the experiments of Ref. [28] involving two components per well and somewhat less closely to the multimode interferometry experiments of Ref. [30]. Depending on the exact configuration, the local modes at each EPR site can be independent, in which case local cross couplings g_{ij} are zero ($g_{12} = 0$), or not independent, as would be the case where the modes are coupled by the BEC self-interaction term, so the couplings cannot be turned off, as in the setup of Ref. [28]. The coupling constant is proportional to the three-dimensional S -wave scattering length, so $g_{ij} \propto a_{ij}$, as in the two-mode case. For example, a typical value of the S -wave scattering length for ^{87}Rb is $a_{11} = 100.4a_0$, where a_0 is a Bohr radius. Zero cross couplings are likely to require spatial separation of the two local modes, as might be achievable with four wells. The quantum dynamics of the four-well Bose-Hubbard model has been studied recently with two different tunneling rates [82].

The Hamiltonian (35) with $\kappa = \kappa_1 = \kappa_2$ is based on the assumption that the second pair of modes a_2, b_2 is coupled between the wells in the same way as the first pair a_1, b_1 , which implies similar diffusion across wells. The case where

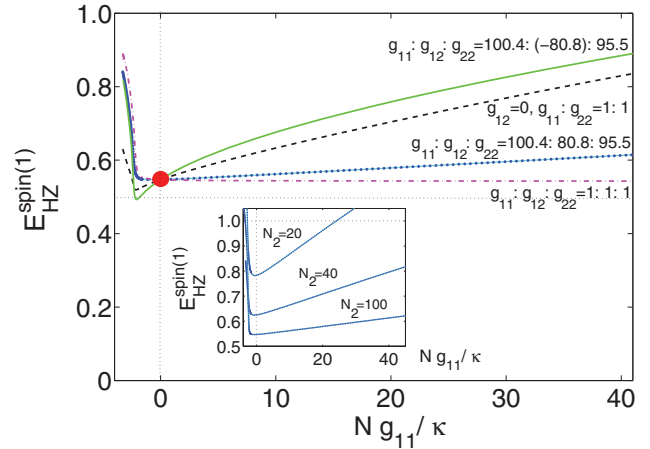


FIG. 14. (Color online) Detecting interwell entanglement using a second local oscillator mode pair: entanglement of the ground state for a two-well potential, at $T = 0$ K, for the four-mode model of Fig. 2, with a variety of local cross couplings g_{ij} , for $N_1 = 5$ and $N_2 = 100$. Here $\kappa = \kappa_1 = \kappa_2 > 0$ and g_{11} is varied with the other values of g_{ij} held in a fixed ratio; $E_{\text{HZ}}^{\text{spin}(1)} < 1$ indicates entanglement and $E_{\text{HZ}}^{\text{spin}(1)} < 0.5$ indicates EPR steering. Curves are labeled in order of nesting as follows: magenta dash dotted curve, equal couplings; blue dotted curve, nonzero cross couplings corresponding to ^{87}Rb Feshbach resonance with $a_{11} = 100.4a_0$, $a_{12} = 80.8a_0$, and $a_{22} = 95.5a_0$; black dashed curve, without cross correlations $g_{12} = 0$ and $g_{22} = g_{11}$; and green solid curve, negative relative cross coupling $g_{11}, g_{12} < 0$. The inset shows the effect of increasingly symmetric atom numbers.

$\kappa_2 = 0$ and $\kappa_1 \neq 0$ is possible where diffusion across the wells can be controlled, as where the local modes represent separate wells. We will examine the predictions for both cases.

2. Symmetric tunneling case

Bose-Einstein-condensate nonlinearity can enhance the entanglement. This is evident on comparing with the case of a zero atom-atom interaction ($g_{ij} = 0$), which corresponds to the result of the linear beam splitter model (Fig. 12) and is indicated by the large red circles in the Figs. 14–16.

First we examine the case of symmetric interwell tunneling with $\kappa = \kappa_1 = \kappa_2$ so there is complete symmetry between the nonlocal setups but a variable local cross coupling g_{12} . Figure 14 shows entanglement using the HZ spin criterion (23) for the ground state for cases of both zero and strong local couplings g_{12} . Asymmetric atom numbers with $N_1 \ll N_2$ are required for the best entanglement, however, as shown in the inset of Fig. 14.

We therefore note from Fig. 14 that the entanglement is improved by using a local oscillator type of approach, in which the second modes a_2 and b_2 are independent of the first at each location ($g_{12} = 0$) [being combined only at the spin measurement stage (19)] and are of much greater numbers ($N_2 \gg N_1$) [19,25]. In addition however, we note from the black dashed curve of Fig. 15 that better entanglement is obtained if the second local oscillator pair a_2, b_2 is also entangled optimally, as given by the critical point of the plots in Fig. 7. Thus the optimal $E_{\text{HZ}}^{(1)}$ is at $N_2 g_{22}/\kappa_2 \approx -2.03$ for modes a_2 and b_2 and at $N_1 g_{11}/\kappa_1 \approx -2.1$ for modes a_1 and b_1

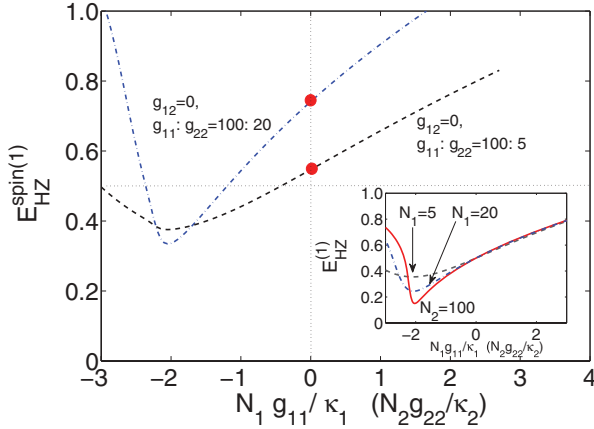


FIG. 15. (Color online) Effect of optimally entangling the second local oscillator mode pair: entanglement of the ground state for a two-well potential, at $T = 0$ K, for the four-mode model of Fig. 2. Here $\kappa = \kappa_1 = \kappa_2$, $g_{12} = 0$, and both g_{11} and g_{22} are varied so that $N_1 g_{11} / \kappa_1 = N_2 g_{22} / \kappa_2$; $E_{\text{HZ}}^{\text{spin}(1)} < 1$ indicates entanglement and $E_{\text{HZ}}^{\text{spin}(1)} < 0.5$ indicates EPR steering. Main graph: black dashed curve, $N_1 = 5$ and $N_2 = 100$; blue dotted curve, $N_1 = 20$ and $N_2 = 100$. The curves are for values of local coupling that optimize $E_{\text{HZ}}^{\text{spin}(1)}$ for each mode pair, in which case for $N_2 \gg N_1$ the $E_{\text{HZ}}^{\text{spin}(1)}$ reaches the value of $E_{\text{HZ}}^{\text{spin}(1)}$ displayed in Fig. 7. The inset reveals the individual degree of HZ entanglement $E_{\text{HZ}}^{\text{spin}(1)}$ for the mode pairs a_1, b_1 and a_2, b_2 , as explained in the text.

(as shown in the inset of Fig. 15). The choice $N_2 g_{22} \sim N_1 g_{11}$ therefore gives enhanced EPR spin entanglement.

The minimum of $E_{\text{HZ}}^{\text{spin}(1)}$ corresponds to the minimum achievable for the HZ entanglement $E_{\text{HZ}}^{\text{spin}(1)}$; this minimum is presented for the case $N_1 = 100$ in Fig. 7. Better entanglement is thus achieved by increasing the number of atoms N_1 provided the other constraints, that $N_2 \gg N_1$ and g_{11} and g_{22} correspond

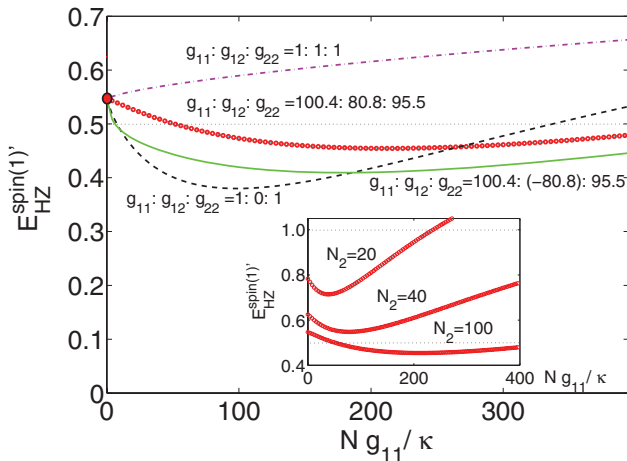


FIG. 16. (Color online) Enhancing entanglement for the repulsive regime: entanglement of the ground state for a two-well potential, at $T = 0$ K, for the four-mode model of Fig. 2. Here $\kappa = \kappa_1 = \kappa_2$. The parameters are the same as for Fig. 14, but the entanglement parameter is calculated for the rotated modes a' and b' of Eq. (32). For large N_2 the strength of the entanglement measure is enough to confirm EPR steering via the criterion (25).

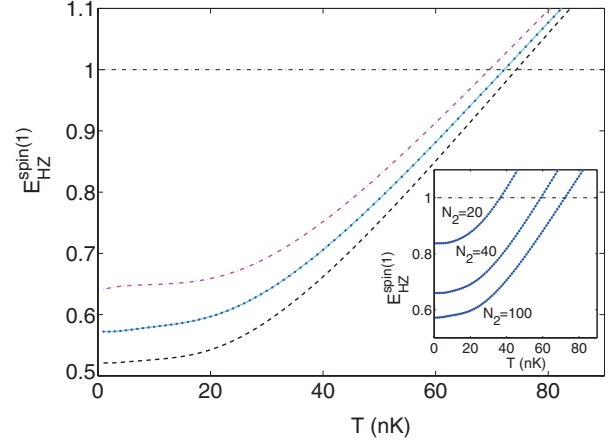


FIG. 17. (Color online) Effect of critical temperatures for the parameters of Fig. 14 when $Ng/\kappa \approx -2.23$.

to the critical choice for each mode pair, are satisfied, as shown in Fig. 15. Analytical details are given in the Appendix.

It is interesting that the case of approximately equal couplings $g_{11} = g_{22} = g_{12}$ is generally less favorable for the HZ spin entanglement (Fig. 14). This can be understood if we rewrite the Hamiltonian (35) in terms of the spin operators. We obtain $H \simeq \chi(J_A^Z)^2 + \chi(J_B^Z)^2 + \kappa(a_1^\dagger b_1 + a_1 b_1^\dagger + a_2^\dagger b_2 + a_2 b_2^\dagger)$, where $\chi \simeq \frac{1}{2}(g_{11} + g_{22} - 2g_{12})$ gives the effective nonlinearity and those terms related to $J_{A,B}^Z$, $N_{1,2}^2$, and $N_{1,2}$ have been omitted. For equal couplings $g_{12} = g_{11} = g_{22}$ the Hamiltonian thus effectively reduces to the linear term of the BS model of Fig. 12, the predictions of which are given by the red circles in Figs. 14 and 15. Furthermore, enhancement of the nonlinearity is possible if g_{12} becomes negative. The green solid curve of Fig. 14 shows an enhanced entanglement for negative local cross coupling $g_{12} < 0$.

Consistent with the two-mode results, the spin HZ entanglement is optimal in the attractive regime $g_{11} < 0$. Enhancement of entanglement in the repulsive regime is possible (Fig. 16) if one examines the spin HZ entanglement for the rotated modes a' and b' of Eq. (32).

The effect of temperature is presented in Fig. 17. In our calculations we account for finite temperatures by assuming a canonical ensemble of $\rho = \exp(-H/k_B T)$ with an interwell coupling of $\kappa/k_B = 50$ nK. The critical temperature for the spin HZ entanglement signature is shown in Fig. 17.

3. Asymmetric tunneling case

An alternative strategy more closely aligned with that used in optics is to consider $\kappa_2 = 0$ and $\kappa_1 \neq 0$. In this case the modes a_2 and b_2 are uncoupled and independent. If they are prepared in coherent states $|\alpha_2\rangle|\beta_2\rangle$ (we set $\alpha_2 = \beta_2 = \alpha$, where α is real), with α large, the entanglement $E_{\text{HZ}}^{\text{spin}(1)}$ approaches the value given in the two-mode case by $E_{\text{HZ}}^{\text{spin}(1)}$. We explain this as follows. For independent modes, as shown by Eq. (A3) of the Appendix, the HZ spin entanglement criterion (20) becomes, upon assuming coherent states for a_2 and b_2 ,

$$|\langle a_1^\dagger b_1 \rangle|^2 \alpha^4 > \langle a_1^\dagger a_1 b_1^\dagger b_1 \rangle (1 + \alpha^2)^2, \quad (36)$$

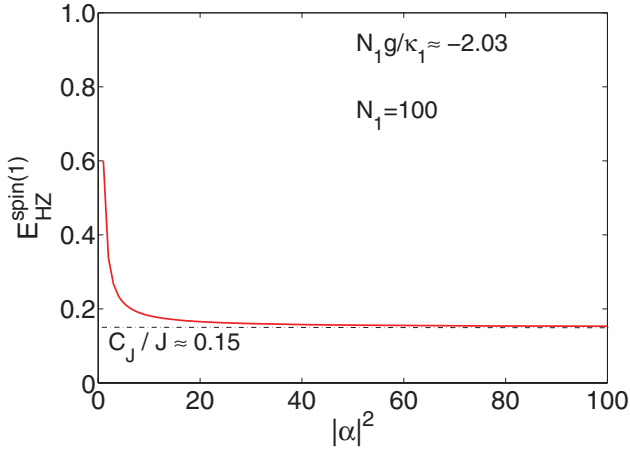


FIG. 18. (Color online) Effect of an uncorrelated coherent atomic oscillator field for mode 2 in a coherent state with amplitude α in the optimal case of Fig. 7 when $N_1 g / \kappa_1 \approx -2.03$.

which will approach the required two-mode entanglement level in the limit of large α . Figure 18 plots the result with finite numbers of atoms for the case of optimal $E_{\text{HZ}}^{(1)}$, which occurs at $N_1 g / \kappa_1 \approx -2.03$ when $N_1 = 100$. We can see that the four-mode EPR entanglement achieved ($C_J / J \approx 0.15$) is that of the two-mode case (Fig. 7) provided there is a large enough number of atoms in the second mode.

VI. CONCLUSION

We have examined two- and four-mode strategies for generating detectable EPR entanglement between groups of atoms in the ground state of a two-well BEC. The two-mode model [47] used to calculate the relevant variances is a simplistic one in view of more recent treatments [71,83], but has been shown to explain experimental data giving evidence of quantum effects, such as squeezing and entanglement, and multiparticle entanglement [27,28,81]. We have developed a version of the Hillery-Zubairy entanglement criterion in the form of a variance and derived from this a condition to observe the nonlocal effect of Einstein-Podolsky-Rosen steering. Furthermore, we have shown that the higher-order HZ entanglement criterion can give information about the number of particles involved in the entangled state and the nature of the multiparticle entanglement.

In order to measure EPR observables locally using Rabi spin rotations and atom number differences we have introduced a second mode for each well or site. Our results reveal that local cross couplings can have a strong effect on entanglement and that, as with the two-mode case, predictions for EPR entanglement and steering improve with higher atom numbers. We find that a spin version of the Hillery-Zubairy entanglement criterion is suited to analyzing the entanglement and the EPR steering paradox in these four-mode experiments.

The predictions in this paper are based on the assumption that the total number N of atoms is fixed. For coherent state inputs, which have a Poissonian number distribution, entanglement at the output of a beam splitter is not possible [84] and we draw the conclusion that number fluctuations can have an important effect on the entanglement depending on

whether post selection and an accurate counting of atoms is possible. The effect of particle fluctuations on entanglement and precision measurement has been studied recently by Hyllus *et al.* [85] and He *et al.* [32,73]. However, we make the final note that these studies have not treated the effect of particle fluctuations on the detection of the EPR steering nonlocality.

ACKNOWLEDGMENTS

This research was supported by an Australian Research Council Discovery and Discovery Early Career Researcher Award grant. We wish to acknowledge useful discussions with M. K. Oberthaler, C. Gross, P. Treutlein, A. I. Sidorov, M. Egorov, and B. Opanchuk. Q.Y.H. wishes to thank the support by the National Natural Science Foundation of China under Grant No. 11121091. P.D.D. wishes to thank the Aspen Center for Physics for their hospitality.

APPENDIX

In this Appendix we show how to directly convert the interwell entanglement shown in Fig. 7 to an EPR entanglement with the use of a local oscillator type of treatment that applies where two of the strong local modes are uncorrelated. This is the case of $g_{12} = 0$, illustrated in Fig. 2.

Local oscillator measurements are achieved optically by combining a mode with a very strong coherent state [6]. We can achieve something effectively equivalent to a local oscillator measurement where the second pair of levels a_2, b_2 is much more heavily populated than levels a_1 and b_1 by assuming that the second pair of modes is in an uncorrelated coherent state. We explain this as follows. Since $J_A^+ = a_1^\dagger a_2$ and $J_A^- = a_1 a_2^\dagger$, and $J_B^+ = b_1^\dagger b_2$ and $J_B^- = b_1 b_2^\dagger$, we can rewrite the criterion (20) in terms of the mode operator moments for this special case by the factorization that is justified for independent fields at each location. Thus

$$|\langle J_A^+ J_B^- \rangle|^2 = |\langle a_1^\dagger b_1 \rangle \langle a_2 b_2^\dagger \rangle|^2 \quad (\text{A1})$$

and similarly

$$\langle (J_A^+ J_A^-)(J_B^+ J_B^-) \rangle = \langle a_1^\dagger a_2 a_1 a_2^\dagger b_1^\dagger b_2 b_1 b_2^\dagger \rangle. \quad (\text{A2})$$

The criterion (20) becomes

$$|\langle a_1^\dagger b_1 \rangle|^2 |\langle a_2 b_2^\dagger \rangle|^2 > \langle a_1^\dagger a_1 b_1^\dagger b_1 \rangle \langle (1 + a_2^\dagger a_2)(1 + b_2^\dagger b_2) \rangle. \quad (\text{A3})$$

Clearly, since the interwell entanglement studied in Sec. IV and summarized in Fig. 7 enables $|\langle a_1^\dagger b_1 \rangle|^2 > \langle a_1^\dagger a_1 b_1^\dagger b_1 \rangle$ via the HZ entanglement criterion, we will have (at least) the same level of four-mode EPR entanglement provided

$$|\langle a_2 b_2^\dagger \rangle|^2 \geq \langle (1 + a_2^\dagger a_2)(1 + b_2^\dagger b_2) \rangle. \quad (\text{A4})$$

In fact, the inequality would represent a violation of the two-site version of the Bell inequality discussed in Ref. [54], which is not achievable for this system. However, it is still possible to optimize the EPR entanglement. This can be achieved in the following way. If the two modes a_2 and b_2 are also coupled via an interwell interaction ($\kappa_2 \neq 0$ in Fig. 2) to produce the ground-state solution of Fig. 9, then $E_{\text{HZ}}^{(1)} < 1$

amounts to $|\langle a_2 b_2^\dagger \rangle|^2 > \langle a_2^\dagger a_2 b_2^\dagger b_2 \rangle$. The optimal $E_{\text{HZ}}^{(1)}$ is at $N_2 g_{22} / \kappa_2 \approx -2.03$, while for the modes a_1 and a_2 the optimal (A3) occurs for $N_1 g_{11} / \kappa_1 \approx -2.1$ (inset of Fig. 15). This

choice gives enhanced EPR entanglement as shown in Fig. 14. Better entanglement is possible for this optimal choice as the numbers are increased (Fig. 15).

-
- [1] A. Einstein, B. Podolsky, and N. Rosen, *Phys. Rev.* **47**, 777 (1935).
- [2] J. S. Bell, *Physics* **1**, 195 (1965); J. F. Clauser, M. A. Horne, A. Shimony, and R. A. Holt, *Phys. Rev. Lett.* **23**, 880 (1969).
- [3] J. F. Clauser and A. Shimony, *Rep. Prog. Phys.* **41**, 1881 (1978).
- [4] A. Aspect, P. Grangier, and G. Roger, *Phys. Rev. Lett.* **49**, 91 (1982); A. Aspect, J. Dalibard, and G. Roger, *ibid.* **49**, 1804 (1982).
- [5] P. G. Kwiat, K. Mattle, H. Weinfurter, A. Zeilinger, A. V. Sergienko, and Y. Shih, *Phys. Rev. Lett.* **75**, 4337 (1995); G. Weihs, T. Jennewein, C. Simon, H. Weinfurter, and A. Zeilinger, *ibid.* **81**, 5039 (1998); W. Tittel, J. Brendel, H. Zbinden, and N. Gisin, *ibid.* **84**, 4737 (2000).
- [6] Z. Y. Ou, S. F. Pereira, H. J. Kimble, and K. C. Peng, *Phys. Rev. Lett.* **68**, 3663 (1992).
- [7] M. D. Reid *et al.*, *Rev. Mod. Phys.* **81**, 1727 (2009); B. Hage, A. Sambrowski, and R. Schnabel, *Phys. Rev. A* **81**, 062301 (2010); Y. Wang *et al.*, *Opt. Express* **18**(6), 6149 (2010); T. Eberle *et al.*, *Phys. Rev. A* **83**, 052329 (2011); A. Sambrowski *et al.*, arXiv:1011.5766v2; S. Steinlechner *et al.*, arXiv:1112.0461v2.
- [8] M. D. Reid, *Phys. Rev. A* **40**, 913 (1989).
- [9] L. Diosi, *Phys. Lett. A* **120**, 377 (1987); R. Penrose, *Gen. Rel. Grav.* **28**, 581 (1996); Stephen L. Adler, *J. Phys. A* **40**, 755 (2007).
- [10] L. C. Lee, *Phys. Rev. Lett.* **97**, 150402 (2006); L. C. Lee *et al.*, *Front. Phys.* **7**, 109 (2012).
- [11] A. K. Ekert, *Phys. Rev. Lett.* **67**, 661 (1991).
- [12] D. J. Wineland, J. J. Bollinger, W. M. Itano, and D. J. Heinzen, *Phys. Rev. A* **50**, 67 (1994).
- [13] M. J. Holland and K. Burnett, *Phys. Rev. Lett.* **71**, 1355 (1993).
- [14] J. P. Dowling, *Phys. Rev. A* **57**, 4736 (1998).
- [15] L. Pezze and A. Smerzi, *Phys. Rev. Lett.* **102**, 100401 (2009).
- [16] G. Y. Xiang *et al.*, *Nature Photon.* **5**, 43 (2011).
- [17] T. Opatrny and G. Kurizki, *Phys. Rev. Lett.* **86**, 3180 (2001); K. V. Kheruntsyan and P. D. Drummond, *Phys. Rev. A* **66**, 031602(R) (2002); K. V. Kheruntsyan, M. K. Olsen, and P. D. Drummond, *Phys. Rev. Lett.* **95**, 150405 (2005).
- [18] A. A. Norrie, R. J. Ballagh, and C. W. Gardiner, *Phys. Rev. Lett.* **94**, 040401 (2005); P. Deuar and Peter D. Drummond, *ibid.* **98**, 120402 (2007).
- [19] A. J. Ferris, M. K. Olsen, E. G. Cavalcanti, and M. J. Davis, *Phys. Rev. A* **78**, 060104 (2008); A. J. Ferris, M. K. Olsen, and M. J. Davis, *ibid.* **79**, 043634 (2009).
- [20] P. Milman, A. Keller, E. Charron, and O. Atabek, *Phys. Rev. Lett.* **99**, 130405 (2007); M. Ogren and K. V. Kheruntsyan, *Phys. Rev. A* **82**, 013641 (2010).
- [21] C. Orzel, A. K. Tuchman, M. L. Fenselau, M. Yasuda, and M. A. Kasevich, *Science* **291**, 2386 (2001).
- [22] M. Greiner, C. A. Regal, J. T. Stewart, and D. S. Jin, *Phys. Rev. Lett.* **94**, 110401 (2005).
- [23] J.-C. Jaskula, M. Bonneau, G. B. Partridge, V. Krachmalnicoff, P. Deuar, K. V. Kheruntsyan, A. Aspect, D. Boiron, and C. I. Westbrook, *Phys. Rev. Lett.* **105**, 190402 (2010); V. Krachmalnicoff *et al.*, *ibid.* **104**, 150402 (2010).
- [24] R. Bücker *et al.*, *Nature Phys.* **7**, 608 (2011).
- [25] C. Gross, H. Strobel, E. Nicklas, T. Zibold, N. Bar-Gill, G. Kurizki, and M. K. Oberthaler, *Nature (London)* **480**, 219 (2011).
- [26] B. Lücke *et al.*, *Science* **334**, 773 (2011).
- [27] J. Esteve *et al.*, *Nature (London)* **455**, 1216 (2008).
- [28] C. Gross, T. Zibold, E. Nicklas, J. Esteve, and M. K. Oberthaler, *Nature (London)* **464**, 1165 (2010).
- [29] M. F. Riedel, P. Böhi, Y. Li, T. W. Hänsch, A. Sinatra, and P. Treutlein, *Nature (London)* **464**, 1170 (2010).
- [30] M. Egorov, R. P. Anderson, V. Ivannikov, B. Opanchuk, P. Drummond, B. V. Hall, and A. I. Sidorov, *Phys. Rev. A* **84**, 021605 (2011).
- [31] N. Bar-Gill, C. Gross, I. Mazets, M. Oberthaler, and G. Kurizki, *Phys. Rev. Lett.* **106**, 120404 (2011).
- [32] Q. Y. He, M. D. Reid, T. G. Vaughan, C. Gross, M. Oberthaler, and P. D. Drummond, *Phys. Rev. Lett.* **106**, 120405 (2011).
- [33] E. Schrödinger, *Naturwissenschaften* **23**, 807 (1935); *Proc. Cambridge Philos. Soc.* **31**, 555 (1935); **32**, 446 (1936).
- [34] H. M. Wiseman, S. J. Jones, and A. C. Doherty, *Phys. Rev. Lett.* **98**, 140402 (2007).
- [35] S. J. Jones, H. M. Wiseman, and A. C. Doherty, *Phys. Rev. A* **76**, 052116 (2007).
- [36] D. J. Saunders *et al.*, *Nature Phys.* **6**, 845 (2010).
- [37] A. J. Bennett *et al.*, arXiv:1111.0739; D. Smith *et al.*, *Nature Commun.* **3**, 625 (2012); B. Wittmann *et al.*, arXiv:1111.0760.
- [38] E. G. Cavalcanti, S. J. Jones, H. M. Wiseman, and M. D. Reid, *Phys. Rev. A* **80**, 032112 (2009).
- [39] S. L. Midgley, A. J. Ferris, and M. K. Olsen, *Phys. Rev. A* **81**, 022101 (2010).
- [40] E. G. Cavalcanti, Q. Y. He, M. D. Reid, and H. M. Wiseman, *Phys. Rev. A* **84**, 032115 (2011).
- [41] L. M. Duan, G. Giedke, J. I. Cirac, and P. Zoller, *Phys. Rev. Lett.* **84**, 2722 (2000).
- [42] R. Simon, *Phys. Rev. Lett.* **84**, 2726 (2000).
- [43] V. Giovannetti, S. Mancini, D. Vitali, and P. Tombesi, *Phys. Rev. A* **67**, 022320 (2003).
- [44] A. Peng and A. S. Parkins, *Phys. Rev. A* **65**, 062323 (2002); Q. Y. He, M. D. Reid, E. Giacobino, J. Cviklinski, and P. D. Drummond, *ibid.* **79**, 022310 (2009); Q. Y. He *et al.*, *Opt. Express* **17**, 9662 (2009).
- [45] B. L. Schumaker and C. M. Caves, *Phys. Rev. A* **31**, 3093 (1985).
- [46] M. D. Reid and P. D. Drummond, *Phys. Rev. Lett.* **60**, 2731 (1988).
- [47] G. J. Milburn, J. Corney, E. M. Wright, and D. F. Walls, *Phys. Rev. A* **55**, 4318 (1997).
- [48] A. Heidmann, R. J. Horowicz, S. Reynaud, E. Giacobino, C. Fabre, and G. Camy, *Phys. Rev. Lett.* **59**, 2555 (1987).
- [49] A. S. Lane, M. D. Reid, and D. F. Walls, *Phys. Rev. Lett.* **60**, 1940 (1988); *Phys. Rev. A* **38**, 788 (1988).

- [50] R. E. Slusher, L. W. Hollberg, B. Yurke, J. C. Mertz, and J. F. Valley, *Phys. Rev. Lett.* **55**, 2409 (1985); M. D. Reid and D. F. Walls, *Phys. Rev. A* **33**, 4465 (1986).
- [51] M. Fernee, P. Kinsler, and P. D. Drummond, *Phys. Rev. A* **51**, 864 (1995); K. Dechoum, P. D. Drummond, S. Chaturvedi, and M. D. Reid, *ibid.* **70**, 053807 (2004).
- [52] F. Gerbier, S. Fölling, A. Widera, O. Mandel, and I. Bloch, *Phys. Rev. Lett.* **96**, 090401 (2006).
- [53] M. Hillery and M. S. Zubairy, *Phys. Rev. Lett.* **96**, 050503 (2006).
- [54] E. G. Cavalcanti, C. J. Foster, M. D. Reid, and P. D. Drummond, *Phys. Rev. Lett.* **99**, 210405 (2007).
- [55] Q. Sun, H. Nha, and M. S. Zubairy, *Phys. Rev. A* **80**, 020101(R) (2009).
- [56] A. Salles *et al.*, *Quant. Inf. Comput.* **10**, 0703 (2010).
- [57] Q. Y. He, E. G. Cavalcanti, M. D. Reid, and P. D. Drummond, *Phys. Rev. A* **81**, 062106 (2010).
- [58] C. V. Chianca and M. K. Olsen, *Opt. Commun.* **285**, 825 (2012).
- [59] R. Hanbury Brown and R. Q. Twiss, *Nature (London)* **177**, 27 (1956); H. J. Kimble, M. Dagenais, and L. Mandel, *Phys. Rev. Lett.* **39**, 691 (1977).
- [60] M. Yasuda and F. Shimizu, *Phys. Rev. Lett.* **77**, 3090 (1996).
- [61] R. Loudon, *Rep. Prog. Phys.* **43**, 913 (1980); M. S. Zubairy, *Phys. Lett. A* **87**, 162 (1982); M. D. Reid and D. F. Walls, *Phys. Rev. A* **34**, 1260 (1986).
- [62] Q. Y. He, P. D. Drummond, and M. D. Reid, *Phys. Rev. A* **83**, 032120 (2011).
- [63] Q. Y. He, S.-G. Peng, P. D. Drummond, and M. D. Reid, *Phys. Rev. A* **84**, 022107 (2011).
- [64] A. S. Sorensen and K. Molmer, *Phys. Rev. Lett.* **86**, 4431 (2001).
- [65] E. G. Cavalcanti and M. D. Reid, *Phys. Rev. Lett.* **97**, 170405 (2006).
- [66] H. F. Hofmann and S. Takeuchi, *Phys. Rev. A* **68**, 032103 (2003).
- [67] G. Toth, *Phys. Rev. A* **69**, 052327 (2004).
- [68] M. Hillery, H. T. Dung, and J. Niset, *Phys. Rev. A* **80**, 052335 (2009).
- [69] H. Zheng, H. T. Dung, and M. Hillery, *Phys. Rev. A* **81**, 062311 (2010).
- [70] M. Hillery, H. T. Dung, and H. Zheng, *Phys. Rev. A* **81**, 062322 (2010).
- [71] D. Ananikian and T. Bergeman, *Phys. Rev. A* **73**, 013604 (2006).
- [72] P. Ribeiro, J. Vidal, and R. Mosseri, *Phys. Rev. Lett.* **99**, 050402 (2007).
- [73] Q. Y. He, T. Vaughan, P. D. Drummond, and M. D. Reid, [arXiv:1111.5117v3](https://arxiv.org/abs/1111.5117v3).
- [74] A. P. Hines, R. H. McKenzie, and G. J. Milburn, *Phys. Rev. A* **67**, 013609 (2003).
- [75] Q. Xie and W. Hai, *Eur. Phys. J. D* **39**, 277 (2006).
- [76] J. I. Cirac, M. Lewenstein, K. Molmer, and P. Zoller, *Phys. Rev. A* **57**, 1208 (1998); G. Mazzarella, L. Salasnich, A. Parola, and F. Toigo, *ibid.* **83**, 053607 (2011); C. Bodet, J. Esteève, M. K. Oberthaler, and T. Gasenzer, *ibid.* **81**, 063605 (2010).
- [77] T. J. Haigh, A. J. Ferris, and M. K. Olsen, *Opt. Commun.* **283**, 3540 (2010).
- [78] J. A. Dunningham and K. Burnett, *J. Mod. Opt.* **48**, 1837 (2001).
- [79] D. Gordon and C. M. Savage, *Phys. Rev. A* **59**, 4623 (1999).
- [80] L. D. Carr, D. R. Dounas-Frazer, and M. A. Garcia-March, *Europhys. Lett.* **90**, 10005 (2010).
- [81] M. D. Reid, Q. Y. He, and P. D. Drummond, *Front. Phys.* **7**, 72 (2012).
- [82] C. V. Chianca and M. K. Olsen, *Phys. Rev. A* **83**, 043607 (2011).
- [83] A. Sinatra and Y. Castin, *Eur. Phys. J. D* **8**, 319 (2000); O. E. Alon, A. J. Streltsov, and L. S. Cederbaum, *Phys. Rev. A* **77**, 033613 (2008); Y. Li, P. Treutlein, J. Reichel, and A. Sinatra, *Eur. Phys. J. B* **68**, 365 (2009); B. J. Dalton and S. Ghanbari, *J. Mod. Opt.* **59**, 287 (2012).
- [84] B. E. A. Salah, D. Stoler, and M. C. Teich, *Phys. Rev. A* **27**, 360 (1983).
- [85] P. Hyllus, L. Pezze, and A. Smerzi, *Phys. Rev. Lett.* **105**, 120501 (2010).